

Overlap Among States at Different Temperatures in the SK Model

Alain Billoire

*Service de physique théorique
CEA Saclay, 91191 Gif-sur-Yvette, France.*

Enzo Marinari

*Dipartimento di Fisica, SMC and UdR1 of INFN and INFN, Università di Roma La Sapienza,
P. A. Moro 2, 00185 Roma, Italy.*

(October 27, 2018)

We discuss the issue of temperature chaos in the Sherrington–Kirkpatrick spin glass mean field model. We numerically compute probability distributions of the overlap among (equilibrium) configurations at two different values of the temperature, both in the spin glass phase. The situation on our medium size systems is clearly non-chaotic, but a weak form of chaos could be emerging on very large lattices.

PACS numbers: 75.50.Lk, 75.10.Nr, 75.40.Gb

Two years after our paper [1] on the subject (that we will quote as **(A)** in the following) we are coming back to the problem of *temperature chaos* in spin glasses and, more widely, in disordered and complex systems. A problem that is, we believe, still a very open one.

In these two years the problem of temperature chaos has been studied under many new lights. One can fairly say that indications are mixed, with some preference for a no-chaos scenario on medium size systems: the detailed discussion of [2] (where arguments against the possibility of a *strong chaos* picture are given) is probably a perfect starting point for the reader interested in the details of the subject.

Perturbation theory in an expansion below T_c (in mean field theory [3]) when pushed to the fifth order shows absence of chaos through highly non-trivial cancelations, although one finds no general feature that could imply that these cancelations will be present at all orders in perturbation theory. The naive TAP equations for the mean field Sherrington–Kirkpatrick model, when solved numerically on systems with order of 10^2 spins, also lead to exclude the presence of temperature chaos [4].

Bouchaud and Sales have shown that there is no chaos in the REM model (but if one sits exactly at T_c) [5]. On the contrary Sales and Yoshino have discussed in [6] the case of DPRM (directed polymers in random media), and have shown that there is temperature chaos in this model, and that a temperature perturbation plays a role very similar for example to a perturbation in the potential: i.e. in the case of DPRM temperature perturbation looks generic and creates chaos. The recent work by Sasaki and Martin [7] describes situations where chaos is present.

These recent studies add new elements to the many former studies of an interesting problem first discussed by Parisi [8], and then studied in many other works (see among others [9–14]). Still the presence or the absence

of temperature chaos is one of the few open problems remaining in the Sherrington–Kirkpatrick model.

Let us start by reminding which were the main results of our first paper **(A)**. There we discussed the behavior of the two-temperature overlap

$$q_{T_1, T_2}^{(2), (N)} \equiv \overline{\left\langle \left(\frac{1}{N} \sum_{i=1}^N \sigma_i^{T_1} \sigma_i^{T_2} \right)^2 \right\rangle} \quad (1)$$

for systems with N spins. The over-line is for the average over the quenched disorder, the brackets are for the thermal average, $\{\sigma_i^{T_1}\}$ is an equilibrium configuration of Ising spins at temperature T_1 , while $\{\sigma_i^{T_2}\}$ is at temperature T_2 . We have considered the Sherrington–Kirkpatrick spin glass mean field model, a diluted finite connectivity mean field spin glass model, and the 3D Edwards–Anderson spin glass. In a T -chaotic situation we would expect $q_{T_1, T_2}^{(2), (N)}$ to go to zero in the infinite volume limit, as soon as $T_1 \neq T_2$. We found however that for all models we studied (on systems with up to 4096 sites) $q_{T_1, T_2}^{(2), (N)}$ was not small for $T_2 - T_1$ finite and reasonably large. To be more precise we found that in our data we had always

$$q_{T_1^{(min)}, T_2}^{(2), (N)} - q_{T_2, T_2}^{(2), (N)} > 0, \text{ for } T_c \geq T_2 > T_1^{(min)} \geq 0.4T_c, \quad (2)$$

even if the value of the l.h.s. was decreasing with increasing volumes. The validity of the relation (2) is suggestive of a very non-chaotic situation (it would hold for an usual ferromagnet), even if from the numerical data of **(A)** it was clear that asymptotically it may well be violated (that is in any case not enough to imply a T -chaotic behavior).

So **(A)** was suggesting a clear absence of chaotic behavior on medium size systems, while showing that for increasing lattice sizes signs of a (modestly) more chaotic behavior were possibly starting to appear. We note here

again that systems with a not huge number of spins can be relevant to the physics of spin glasses. The experiments of reference [15] show that the number of spin involved in the collective behavior observed in a typical spin glass experiment is of the order of 10^5 , that is not so far away from the number of spins we can handle numerically today. Accordingly, even if it should emerge that T -chaos is asymptotically present for very large volumes, the present numerical simulations could turn out to describe reasonably well the experimental regime.

In order to get further informations on the sensitivity of the spin glass phase with respect to temperature, we have decided to measure the full probability distribution of the overlap of configurations equilibrated at different values of the temperature: $P_{T_1, T_2}(q)$ (In (A) we restricted ourselves to the second moment of this distribution). In terms of $P_{T_1, T_2}(q)$, temperature chaos just means that $\lim_{N \rightarrow \infty} P_{T_1, T_2}(q) = \delta(q)$, for any $T_1 \neq T_2$. A more complete information like the one contained in the full probability distribution of the order parameter can indeed allow a more detailed analysis of the scaling behavior, making possible to uncover a wider range of phenomena.

Since the three models studied in (A) were showing a very similar behavior, we focus here on one of them, namely the Sherrington–Kirkpatrick model.

The numerics are very similar to the ones of (A), and we refer to [1] for a discussion of the details of the simulations. We use binary quenched random couplings, $J = \pm 1$. Here we have studied systems with $N = 64$, $N = 256$, $N = 1024$ and $N = 4096$ spins, down to $T = 0.4 = 0.4 T_c$. We have used a multi spin (different spins are encoded in the same computer word) version [16] of the parallel tempering Monte Carlo algorithm. Two copies of the system at each one of a set of temperature values ($0.4, 0.4 + \Delta T, 0.4 + 2\Delta T \dots$, with $\Delta T = 0.025$ but for $N = 4096$ where $\Delta T = 0.0125$) are brought to equilibrium (in the same realization J of the couplings) and are used to compute the $P_{T_i, T_j}^{(J)}(q)$ (more precisely the subset with temperatures $0.40, 0.45, 0.50, \dots$). An average over 1024 different realizations of the quenched disorder (256 for $N = 4096$) is taken to compute the average $P_{T_i, T_j}(q)$. This is an order of magnitude more disorder samples than in [1]. For each realization we have performed 400K sweeps for equilibrium plus 1000K sweeps for measurements (520K only for $N = 4096$).

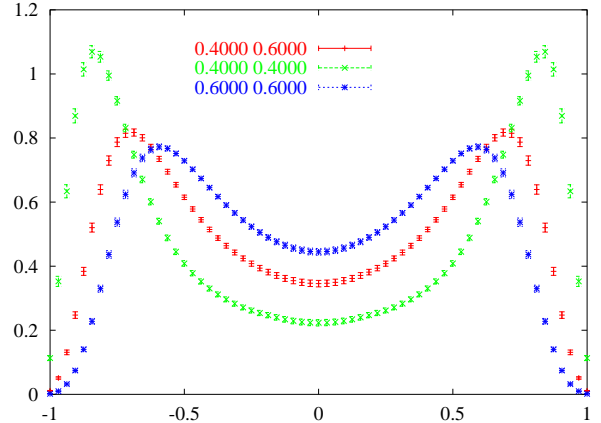


FIG. 1. $P(q)$ in a non-diagonal case ($T_1 = 0.4$ and $T_2 = 0.6$) and for the two corresponding diagonal cases ($T_1 = T_2 = 0.4$ and $T_1 = T_2 = 0.6$). Here $N = 64$.

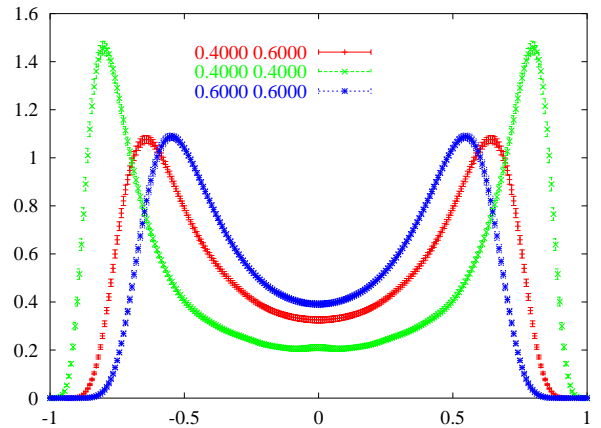


FIG. 2. As in figure 1 but for $N = 256$.

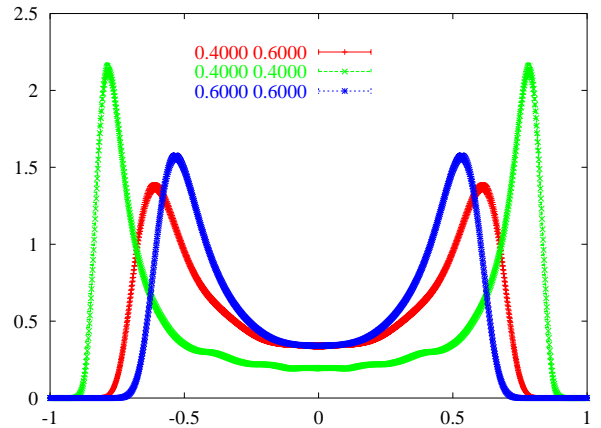


FIG. 3. As in figure 1 but for $N = 1024$.

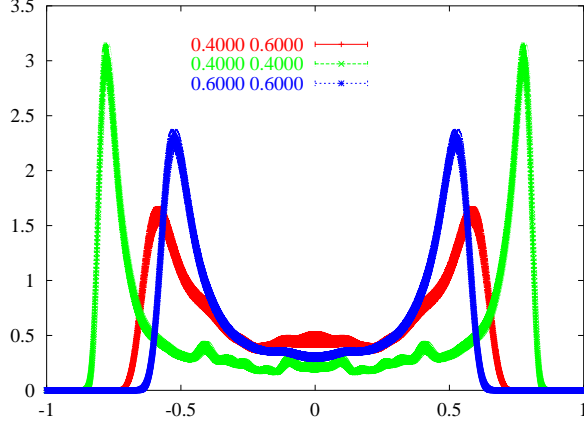


FIG. 4. As in figure 1 but for $N = 4096$.

We show at first the probability distributions themselves (normalized by $\int_{-1}^1 P(q) dq = 1$). These distributions have been symmetrized, although they are quite symmetric, even sample by sample. In each of figures 1, 2, 3 and 4 we show three $P_{T_1, T_2}(q)$: the non-diagonal one that gives the probability of the overlap of configurations at $T = 0.4$ (the lower temperature we equilibrate) with configurations at $T = 0.6$, and the two diagonal probability distributions with $T_1 = T_2 = 0.4$ and $T_1 = T_2 = 0.6$ respectively. In figure 1 we have data from our smallest lattice with $N = 64$, in figure 2 from $N = 256$, in figure 3 from $N = 1024$, and in figure 4 we have data from the largest lattice, with $N = 4096$.

On the smallest lattice (figure 1) the peak of the non-diagonal $P(q)$ is higher than the one of $P_{0.6, 0.6}$, and its position is basically at half way between the positions of the maxima of $P_{0.4, 0.4}$ and $P_{0.6, 0.6}$. This is typically what would happen in a ferromagnet. For increasing volumes the position of this peak is moving (very slowly) to lower values of q , but does not seem to approach $q = 0$ (we will discuss in detail this point in the following).

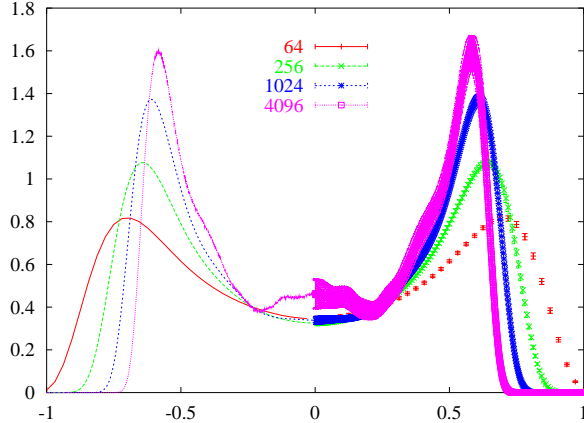


FIG. 5. $P(q)$ for the non-diagonal case only ($T_1 = 0.4$ and $T_2 = 0.6$) for different lattice volumes. For giving more information about the actual form of the measure curves we only plot errors in the $q > 0$ part of the plot.

In figure 5 we show in the same plot the four non-diagonal $P_{0.4, 0.6}$ for $N = 64, 256, 1024$ and 4096 . These $P_{0.4, 0.6}(q)$ are normalized and are drawn on the same scale, so that a visual comparison of the four curves is meaningful. Here we see that the $q \neq 0$ peak of $P_{0.4, 0.6}(q)$ do increase as function of N (but for a negative analysis of this statement see later in the text and figure 7), and that its position shifts only very little towards $q = 0$. The mass carried by the distribution $P(q)$ in $q \approx 0$ seems to be increasing on the largest lattice, but this effect is affected by a large statistical error. Figure 4 shows indeed wiggles in $P_{0.4, 0.4}(q)$ that are known not to exist in the infinite volume limit, and are accordingly to be attributed to the limited number of disorder samples. The bump popping up around $q = 0$ in figure 5 is compatible with the statistical error. It is not visible in our data for larger T_1 values ($0.45, 0.50, \dots$).

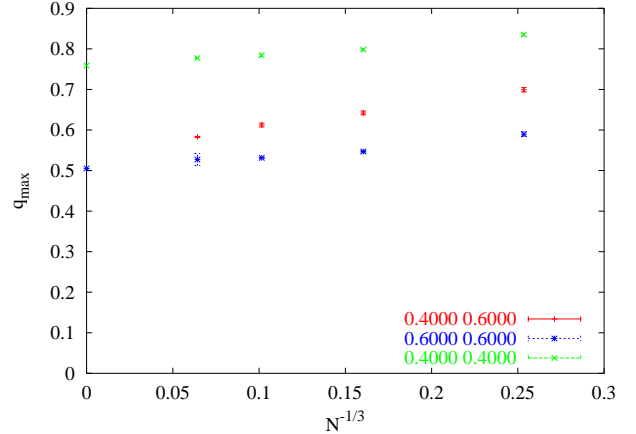


FIG. 6. The values of q where $P(q)$ is maximum, q_{\max} , for the diagonal and non-diagonal $P(q)$ as function of $N^{-1/3}$.

In figure 6 we plot the values of q where $P(q)$ is maximum, q_{\max} , for the diagonal and non-diagonal $P(q)$ at different N values. The two points at $N = \infty$ for $P_{0.4, 0.4}(q)$ and $P_{0.6, 0.6}(q)$ have been obtained [17] using the method of [18]: they show how reliable is a linear fit in $N^{-1/3}$ of our data for the diagonal distributions. The points for $P_{0.4, 0.6}(q)$ show some curvature, but the effect is not dramatic, and a non-zero value in the limit $N \rightarrow \infty$ is surely favored.

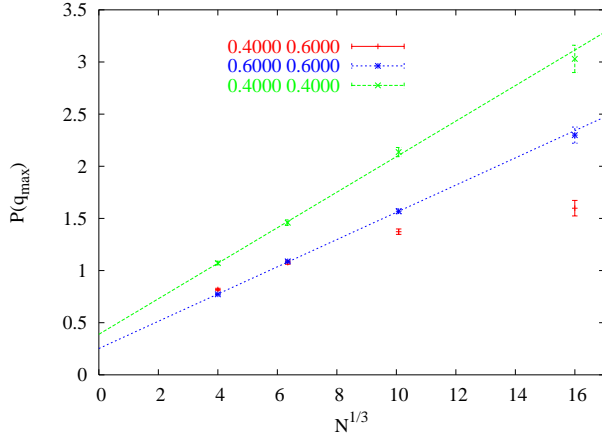


FIG. 7. $P(q_{\max})$ as a function of $N^{1/3}$ for the three different $P(q)$.

As we have already shown, the peaks of the (temperature) non-diagonal $P(q)$ increase when N increases, but not as fast as the ones of the diagonal $P(q)$. In figure 7 we show the value of $P(q_{\max})$ for the different N values and for the three $P(q)$ we are discussing. The height of the peaks of the two diagonal $P(q)$ increases exactly like $N^{1/3}$ as it should. The two continuous straight lines are the best linear fit to the diagonal data: the fits turn out to be very good.

From figure 7 the situation of $P_{0.4,0.6}(q)$ looks quite different. Here the growth slows down at $N = 1024$ and is really small on our largest lattice size with $N = 4096$. We do not believe that one can draw precise quantitative conclusions from figure 7: a (weak) non-chaotic picture could survive in the infinite volume limit, or chaos could appear very slowly (only on very large volumes). Let us spell clearly, in any case, that the mechanism that will govern a possible appearance of chaos will be based on the $P_{T_1, T_2}(q)$ having two $q = 0$ and and at $q = q^* > 0$, and by having the $q = 0$ peak growing for increasing volume at the expense of the q^* peak. In any case our numerical results appear to support the idea that temperature chaos will not be effective on the typical sizes that are relevant in spin glass experiments [15].

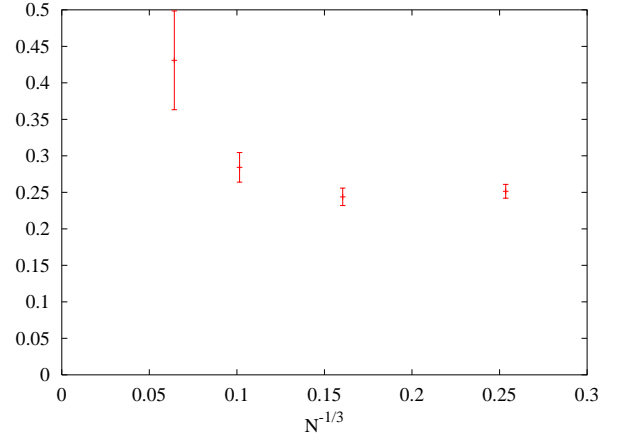


FIG. 8. \mathcal{R} as defined in equation (3) as a function of $N^{-1/3}$.

In order to be more quantitative we have also looked at the ratio of the mass carried by $P_{0.4,0.6}(q)$ close to $q = 0$ as compared to the mass carried by the large q region. We define

$$\mathcal{R} \equiv k \frac{\int_{-m}^{+m} P(q) dq}{\int_{q_{max}}^1 P(q) dq}, \quad (3)$$

where k is a normalization constant, and we take $m = 0.05$ (a very similar picture would be obtained for any m not too large). \mathcal{R} decreases with N if the mass of the peaks at large q dominates, while it increases when the dominating contribution is the one at $q \approx 0$.

We plot \mathcal{R} for $P_{0.4,0.6}(q)$ versus $N^{-1/3}$ in figure 8. \mathcal{R} is constant on the smaller lattices, but starts increasing on the largest lattice size. The error due to sample to sample fluctuations is here very large (the simulation at $N = 4096$ have been very costly in computer time), and the growth of \mathcal{R} is not significant at more than two standard deviations, but an effect is very plausibly there. Again, this is probably an indication toward the fact that temperature chaos could eventually emerge on very large systems.

It is worth noticing that if temperature chaos is (slowly) emerging when increasing N this is probably not happening with the position of the two peaks at large $|q|$ shifting to $q = 0$, but with a third peak in $q = 0$ emerging and eventually becoming the only contribution, and accordingly a discontinuity in q_{\max} as function of $N^{-1/3}$ (Figure 6).

The problem of temperature chaos, already at the mean field level, is turning out to be a hard problem: this is true both for analytical and for numerical computations. Here we have provided some further hints about the behavior of the system in the infinite volume limit: the very large scale, state of the art simulations we have been able to run, give some suggestions, probably hinting in favor of a very weak chaos that would emerge only for very large lattice sizes.

We acknowledge many enlightening discussions with Giorgio Parisi and Silvio Franz. We thank Andrea Crisanti and Tommaso Rizzo for providing us with the $N = \infty$ data for q_{\max} for the diagonal $P(q)$ of figure 6. The numerical simulations have been run on the CEA Compaq Alpha Server at Grenoble.

-
- [1] A. Billoire and E. Marinari, J. Phys. A: Math. Gen. **33** L265, 2000, preprint cond-mat/9910352.
 - [2] J.-P. Bouchaud, V. Dupuis, J. Hammann and E. Vincent, Phys. Rev. B **65**, 024439 (2002).
 - [3] T. Rizzo, J. Phys. A: Math. Gen. **34**, 5531 (2001).
 - [4] R. Mulet, A. Pagnani and G. Parisi, Phys. Rev. B **63**, 184438 (2001).
 - [5] J.-P. Bouchaud and M. Sales, Europhys. Lett. **56**, 181 (2001), preprint cond-mat/ 0105151.
 - [6] M. Sales and H. Yoshino, Phys. Rev. E **65**, 066131 (2002), preprint cond-mat/0112384.
 - [7] M. Sasaki and O. Martin, preprint cond-mat/0204413; cond-mat/0206316.
 - [8] G. Parisi, Physica A **124**, 523 (1984).
 - [9] I. Kondor, J. Phys. A: Math. Gen. **22**, L163 (1989).
 - [10] M. Ney-Nifle and H. J. Hilhorst, Physica A **193**, 48 (1993).
 - [11] I. Kondor and A. Végö, J. Phys. A: Math. Gen. **26**, L641 (1993).
 - [12] F. Ritort, Phys. Rev. B **50**, 6844 (1994).
 - [13] S. Franz and M. Ney-Nifle, J. Phys. A: Math. Gen. **28**, 2499 (1995).
 - [14] M. Ney-Nifle, Phys. Rev. B **57**, 492 (1998), preprint cond-mat/9707172.
 - [15] Y. G. Joh et al., Phys. Rev. Lett. **82**, 438 (1999), preprint cond-mat/9809246.
 - [16] H. Rieger, HLRZ 53/92, hep-lat/9208019; our code is based on F. Zuliani (1998), unpublished.
 - [17] A. Crisanti and T. Rizzo, private communication.
 - [18] A. Crisanti and T. Rizzo, preprint cond-mat/0111037.